Systematic Design and Simulation of a Miniaturized Conical Log-Spiral Antenna

Ali Araghi and Lai Bun Lok
Department of Electronic and Electrical Engineering, University College London, London, U.K.
{a.araghi, l.lok}@ucl.ac.uk

***Abstract* — This paper presents a systematic method to design an electrically-small conical log-spiral antenna (CSA). The design is based on a thin flexible printed dielectric substrate to form the cone surface, and then a resistor is added between the spiral arms at the larger diameter end of the antenna. To demonstrate the proposed approach, a 2-arm CSA is designed and simulated. The minimum operating frequency of the CSA is reduced from 1.02 GHz to 0.8 GHz. A microstrip balun is designed to differentially excite the CSA. The final antenna has a fractional impedance bandwidth of 121% (0.8-3.27 GHz) with return loss better than 10 dB. The axial ratio of the antenna is also assessed to show its circularly polarized performance within the operating bandwidth.**

***Keywords* — Conical log-spiral antenna, balun, circular polarization.**

I. Introduction

Spiral antennas are a class of frequency-independent circularly polarised radiating structures that can be formed by two conductive spiral arms, growing in archimedean or logarithmic fashion [1]. The frequency-independence property in antennas refers to the case where its radiation pattern and input impedance are non-varying beyond a lower operating frequency limit of interest. This is achieved by considering the *angle principle* and the *truncation principle* [2], [3]. The angle principle is the case where antenna performance is mainly governed by the angles of its geometry. This means that if the shape of the antenna is entirely specified by angles, all dimensions are increased by a constant factor, leading to relatively fixed radiation and impedance if the frequency is also increased by that constant factor. In other words, the performance is theoretically independent of frequency if the antenna's dimensions are held constant. As this theoretical antenna is infinitely large by definition, the truncation principle must also be taken into account. This leads to the identification of a finite "active region", also known as the effective radiating aperture, that is responsible for radiation at the operating frequencies of interest. Subsequently, this constrains the lateral dimensions of the spiral antenna which approximately occurs when the circumference of the spiral equals one wavelength at the lowest desired frequency.

The conventional planar spiral antenna provides a bi-directional radiation pattern normal to the antenna's horizontal plane. In some real-world scenarios, a single directional lobe is preferred which means the other lobe acts as a strong undesired back lobe. To address this issue, planar spiral antennas are usually designed with a cavity on one side which can be filled with electromagnetic absorber layers to mitigate the back lobe. Such a structure is called a cavity-backed spiral antenna [4]. Under this circumstance, the aperture is employed in an inefficient way as half of the radiating energy is suppressed.

When a pair of equiangular spirals is wrapped around a cone, the conical log-spiral antenna (CSA) is formed. This antenna radiates predominantly toward the apex in a unidirectional manner. The physical characteristics of the cone in CSAs offer additional design parameters compared to the planar spiral which bring more degrees of freedom to the design procedure. The lowest operating frequency is still governed by the circumference of the largest lateral cut which is where the cone is truncated.

Although several research works have been conducted on CSAs [5], [6], [7], [8], [9], the achievable minimum operating frequency remains an area that has received little attention. A miniaturized CSA is presented in [10] with a physically long impedance transformer that increases the final size of the assembled structure. A complex geometry with several resistors at each arm of a CSA is proposed in [11] to make the structure compact. A small-size antenna is designed in [12] which provides relatively low impedance bandwidth. Genetic algorithms are used in [13] to reduce the size of a coiled conical helix which results in a complex geometry. In this work, we present a systematic approach to designing a miniaturized CSA by applying a thin flexible PCB substrate to form the cone surface with a resistor connected between the tip of the arms at the large end of the cone.

II. Miniaturized Conical Log-Spiral Antenna

We first briefly explore the conventional CSA design procedure, and then a systematic method is proposed to reduce the lowest operating frequency and achieve a miniaturized structure for the CSA.

A. Conventional CSA Design

The overall geometry of a left-handed conical log-spiral arm and its governing design parameters are shown in Fig. 1 (a). This geometry is characterised by design parameters comprising of the cone's half angle θ, the wrap angle α, and the angular width of the arm δ. The cone is truncated to a height of H with the small and large ends having diameters of d and D respectively. The edges of the arm are specified by two spiral curves (see Fig. 1 (a)). The design procedure begins with defining one of these curves as:

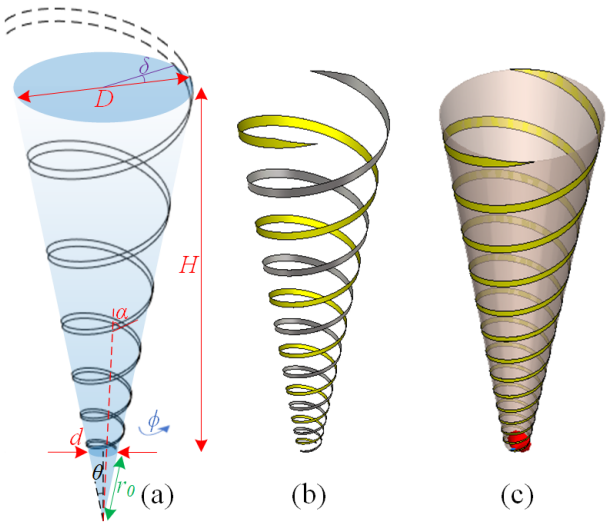

Fig. 1. (a) The geometrical parameters of a conical log-spiral arm, (b) Two-arm conical log-spiral antenna (CSA), (c) CSA on a flexible dielectric substrate excited by a discrete port (red dot) from the small end for simulation purposes only.

$$r_1 = r_0 e^{a\phi}, \tag{1}$$

with the expansion factor of $a = \sin\theta/\tan\alpha$ and then, the other curve is expressed as:

$$r_2 = r_0 e^{a(\phi-\delta)}. \tag{2}$$

These curves set the edges of a conductive strip for one spiral arm of the CSA. The resultant CSA is formed by rotating this arm $180°$ along its axis to make two conductive strips wound around the surface of the truncated cone as shown in Fig. 1 (b). This yields left-handed circularly polarized (LHCP) radiation along the virtual apex of the cone when used as a transmitting antenna. For applications in radar, such an antenna will drastically attenuate RHCP waves. Therefore, a pair of CSAs are typically used in practical scenarios involving specular targets and have identical parameters with opposite polarization i.e. one antenna is LHCP, the other antenna is RHCP.

Considering the operating frequency range of interest, it is possible to approximate the diameter of the cone ends by $d \approx \lambda_{\min}/4$ and $D \approx 3\lambda_{\max}/8$ where $\lambda_{\min}$ and $\lambda_{\max}$ are wavelengths of the high and low operating frequencies respectively. However, a correlation exists between the band edges and the magnitude of near-field current along the CSA [3]. This correlation is empirically tabulated as diameter-to-wavelength ratios of the circles truncating the cone with respect to the active region as a function of α and θ [14]. Therefore, the cone's physical characteristics, as well as other geometrical parameters of conventional CSAs are often determined by the approach of [14] to achieve an initial design.

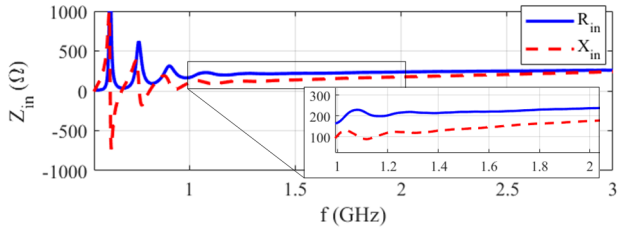

Fig. 2. Input impedance of the designed DW CSA excited by a discrete port.

B. *Systematic Method to Design Miniaturized CSA*

We now aim to design a conventional CSA and reduce its lowest operating frequency to yield an electrically-small antenna. To this end, our method can be summarized as follows:

#1: Determine the geometry of a conventional 2-arm CSA using the method in [14] for a given frequency range. This is the case where spiral arms are wrapped around the trajectory of a hollow cone, which is called "air CSA" hereinafter.

#2: Apply a thin flexible substrate with a relatively high dielectric constant to cover the surface of the hollow cone. This will enhance the bandwidth and will reduce the lower frequency. We call this structure "dielectric-wrapped (DW) CSA". At this step, the structure is excited by a discrete port with an arbitrary impedance in a full-wave simulator.

#3: The input impedance $Z_{\text{in}} = R_{\text{in}} + jX_{\text{in}}$ of the design will then be read versus frequency. The value of R_{in} should be stabilized around an average value of R_{ave} beyond a specific frequency. Then, an ideal resistance of $R_{\text{L}} = R_{\text{ave}}$ is inserted between the arms of the DW CSA at its large end. This reduces the lower frequency even further. The reason for this will be explained in Section III. Let us call this structure "Resistive-loaded (R)DW CSA".

#4: Design a balanced-to-unbalanced (balun) impedance transformer to differentially excite the designed RDW CSA.

Considering steps #1 and #2 above, the CSA arms are designed to be wrapped around on a thin flexible standard substrate with thickness of 0.63 mm and $\epsilon_r = 10.7$. The structure is excited with a discrete port as shown in Fig. 1 (c) with $D = 9.36$ cm, $d = 1.38$ cm, $H = 22.6$ cm, $\alpha = 75°$, $\theta = 10°$, and $\delta = 30°$.

Regarding step #3, Z_{in} of the designed DW CSA is presented in Fig. 2. Across the frequency range of study, it is observed that R_{in} is relatively constant above 1 GHz with $R_{\text{ave}} = 213\ \Omega$. Therefore, a resistance R_{L} equal to R_{ave} is added to the structure.

A tapered microstrip balun is designed (step # 4) to be printed on a standard substrate with $\epsilon_r = 2.2$ as shown in Fig. 3 (a), (b), and (c) from different angles with physical parameters of $h = 0.157$ cm, $w_f = 0.49$ cm, $w_p = 0.14$ cm,

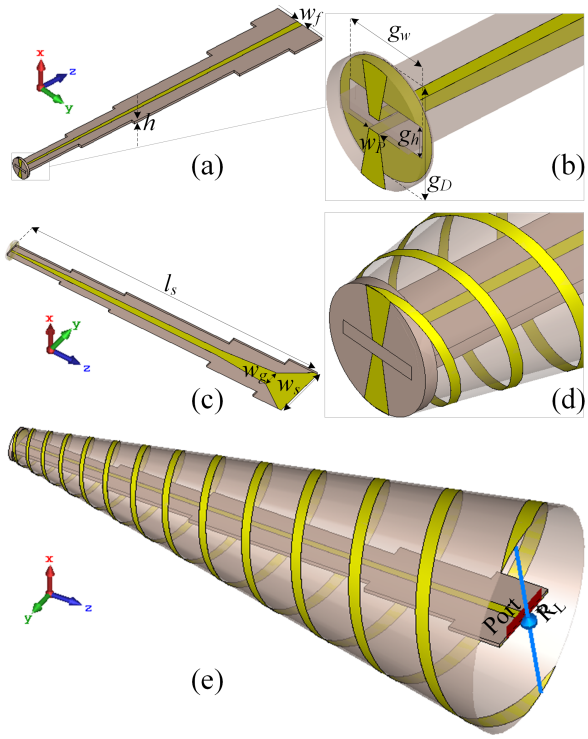

Fig. 3. (a) The designed balun from the topside angle, (b) the circular PCB at the balanced end: the conductive lines are shown solid and the PCB substrates are transparent for illustrative purposes only. (c) The balun from the backside angle. (d) The spiral arms are connected to the balanced lines at the small end. (e) The final designed structure (RDW CSA) with R_{L} added between the arms at the large end.

$g_w = 1.04$ cm, $g_h = 0.36$ cm, $g_D = 1.32$ cm, $w_s = 4$ cm, $w_g = 1.2$ cm, $l_s = 22.43$ cm. The balun contains a circular PCB perpendicularly attached to the small end (Fig. 3 (b)) which is used to connect the balanced lines to the spiral arms as presented in Fig. 3 (d). The final designed RDW CSA with the R_{L} connected between the spiral arms at the large end is shown in Fig. 3 (e).

According to [14], an air CSA with such geometry exhibits a theoretical frequency range of 1 GHz to 3 GHz. In this case, the balun must be modified with $w_p = 0.04$ cm; otherwise, the structure cannot be appropriately matched within its theoretical operating frequency range.

III. Results and Discussions

The simulated S_{11} of the designed CSAs are shown in Fig. 4. This shows the input impedance frequency responses are achieved with the proposed systematic method to design an electrically-small CSA. It demonstrates that employing the dielectric substrate reduces the minimum operating frequency of $f_{\min} = 1.02$ GHz for the air CSA[1] so that the DW CSA has a minimum operating frequency of $f_{\min} = 0.9$ GHz with respect to -10 dB of S_{11}. Adding R_{L} mainly impacts the performance at the lower frequencies which reduces the

[1]Note that a resonance occurs at around 0.9 GHz for the air CSA which is magnified in the inset of Fig. 4. However, this is too narrow to be considered as the minimum frequency of operation for an ultra-wideband structure.

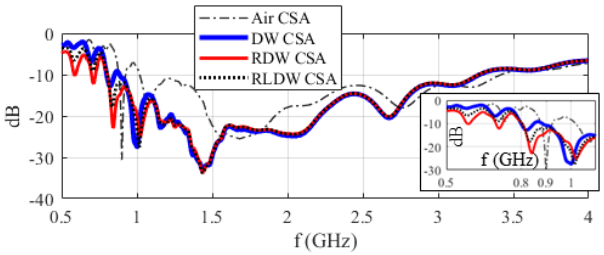

Fig. 4. S_{11} of the designed CSAs.

minimum frequency further to $f_{\min} = 0.8$ GHz for the RDW CSA. This is due to the radiation mechanism of the CSA where the large end governs its performance at low frequency. Hence, S_{11} at relatively higher frequencies show an almost similar response for both DW and RDW CSAs with the maximum operating frequency of $f_{\max} = 3.27$ GHz which provides 121% fractional bandwidth for the RDW CSA design.

Compared to the air CSA, the designed RDW CSA reduces $f_{\min}$ more than 20% from 1.02 GHz to 0.8 GHz with the same physical size.

Note that the following should be taken into consideration when realizing the RDW CSA in practice:

- It is first required to unwrap the arms to transform them from a three dimensional geometry to a planar version. To this end, transformation functions can be applied [15], [16], [17]. Then the unwrapped spiral arms is printed on a flexible substrate via standard PCB manufacturing techniques. The PCB must then be wrapped to form the desired conical 3D structure.
- The designed balun is fabricated on two PCBs as explained in Section II where the conductive strips must be soldered to each other and to the spiral arms at their intersections (see Fig. 3 (b) and (d)).
- To connect R_{L} to the spiral arms at the large end, its pins must be soldered to two pieces of standard wires and then the other end of wires are soldered to the arms. For the case where two 4 cm length 25-gauge wires are employed, the corresponding self-inductance of each wire is $L_{\mathrm{s}} = 40.2$ nH [18]. Hence, two L_{s} inductance are added to R_{L} in series to create a more realistic simulation. This structure is named RLDW CSA with the S_{11} reported in Fig. 4 for comparison purposes. This result shows the inclusion of L_{s} of this value does not significantly alter $f_{\min}$ for the antenna.

The frequency response of the designed CSAs are replotted as the inset of Fig 4 for lower frequency bands to provide a better comparison. It can be seen that the radiation characteristics of RDW CSA show no substantial difference with RLDW CSA in our simulations.

The radiation pattern of the designed RDW CSA is presented in Fig. 5 for different frequencies. The realized gain at $f_{\min} = 0.8$ GHz is 4.02 dBi which is lower than that of other frequencies. This is because of the impact of R_{L} on the radiation and total efficiencies of the antenna in the lower

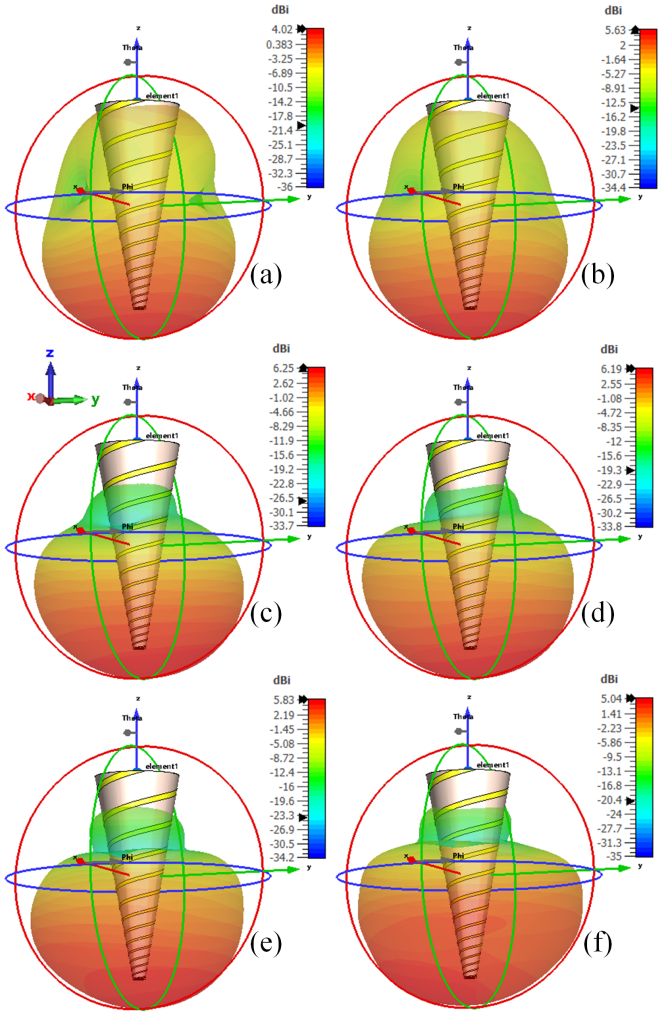

Fig. 5. The realized gain radiation pattern of the designed RDW CSA at (a) 0.8 GHz, (b) 0.9 GHz, (c) 1.5 GHz, (d) 2 GHz, (e) 2.5 GHz, (f) 3 GHz.

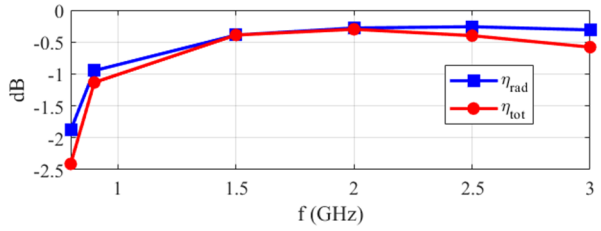

Fig. 6. Radiation and total efficiencies versus frequency.

bands. So, the size reduction is accompanied by a drop in gain. This trade-off is common in miniaturized antennas [19]. The maximum simulated antenna realized gain is 6.25 dBi which is obtained at $f = 2$ GHz. The radiation and total efficiencies of the RDW CSA are presented in Fig. 6 as a function of frequency.

The axial ratio (AR) of the designed RDW CSA is shown in Fig. 7 at some frequencies of interest. The regions where AR $\leq$ 3 dB represent the spatial angles that the antenna generates

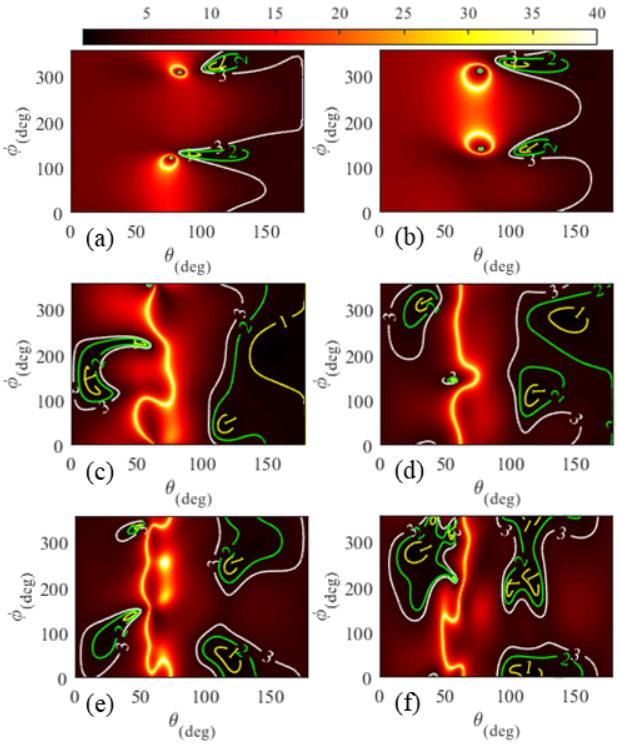

Fig. 7. The axial ratio (AR) of the designed RDW CSA at (a) 0.8 GHz, (b) 0.9 GHz, (c) 1.5 GHz, (d) 2 GHz, (e) 2.5 GHz, (f) 3 GHz. The colorscale is in dB.

Table 1. Comparison Between Our Structure and Other Works

Ref.	Gain (dBi) at $f_{\min}$	Size reduction	Fractional bandwidth	Geometrical complexity
[11]	-10	10%	120%	High
[12]	< 5	N.R.	44%	Moderate
[13]	-15	30%	163%	Very high
This work	4.02	$> 20\%$	121%	Moderate

circularly polarized radiation. In conjunction with Fig. 5, it is revealed that the antenna exhibits circular polarization mainly along its front beam, as desired.

A comparison between our work and other miniaturized CSAs is presented in Table 1. This shows that our work offers a gain at $f_{\min}$ which is much higher than that of [11], [13] while the structure in [12] has a higher gain at its corresponding $f_{\min}$ compared to our work, however, its fractional bandwidth is limited which is a reason of achieving such a high gain at $f_{\min}$. The operational bandwidth of [13] is more than our work with a higher reduction in size but with the cost of severe loss in gain and a very high level of complexity in geometry. Overall, our proposed structure offers a moderate level of complexity with a relatively high gain at $f_{\min}$ and reasonable values of size reduction and fractional bandwidth.

IV. Conclusion

A miniaturized UHF conical log-spiral antenna is designed and simulated in this paper. To this end, a systematic method is employed to reduce its lower operating frequency. The method

is based on utilizing a flexible substrate to form the cone and a resistor is connected between the spiral arms at the large end of the cone. The simulation results show that the antenna lower frequency is reduced by more than 20%. The final structure has a $S_{11} < -10$ dB response for frequencies between $0.8-3.27$ GHz. The axial ratio pattern of the structure is also reported at different frequencies of operation.

REFERENCES

[1] C. A. Balanis, *Antenna theory: analysis and design*. John wiley & sons, 2016.

[2] V. Rumsey, "Frequency independent antennas," in *1958 IRE International Convention Record*, vol. 5. IEEE, 1966, pp. 114–118.

[3] J. Dyson, "The characteristics and design of the conical log-spiral antenna," *IEEE transactions on antennas and propagation*, vol. 13, no. 4, pp. 488–499, 1965.

[4] C. Baard, Y. Liu, and N. Nikolova, "Ultra-wideband low-cost high-efficiency cavity-backed compound spiral antenna," *Electronics*, vol. 9, no. 9, p. 1399, 2020.

[5] A. J. Ernest, Y. Tawk, J. Costantine, and C. G. Christodoulou, "A bottom fed deployable conical log spiral antenna design for cubesat," *IEEE Transactions on Antennas and Propagation*, vol. 63, no. 1, pp. 41–47, 2014.

[6] T. W. Hertel and G. S. Smith, "Analysis and design of two-arm conical spiral antennas," *IEEE transactions on electromagnetic compatibility*, vol. 44, no. 1, pp. 25–37, 2002.

[7] S. Yao, X. Liu, and S. V. Georgakopoulos, "Morphing origami conical spiral antenna based on the nojima wrap," *IEEE Transactions on Antennas and Propagation*, vol. 65, no. 5, pp. 2222–2232, 2017.

[8] P. Piksa, "Parametric study on conical log-spiral antenna," in *2009 3rd European Conference on Antennas and Propagation*. IEEE, 2009, pp. 3340–3342.

[9] T. Pan, L. Dai, S. Chen, Z. Yan, and Y. Lin, "Low-impedance flexible archimedean-equiangular spiral antenna," *IEEE Antennas and Wireless Propagation Letters*, vol. 18, no. 9, pp. 1789–1793, 2019.

[10] A. Gu, S. Yang, and Z. Nie, "Analysis and design of miniaturized ultra-wideband conical log spiral antennas," in *2013 Cross Strait Quad-Regional Radio Science and Wireless Technology Conference*. IEEE, 2013, pp. 191–194.

[11] H.-s. Youn, N. Celik, M. Iskander, J. Baker, J. Graham, and S. Murphy, "Miniaturized conical spiral antenna with tapered resistive roading and corrugated arms," in *2011 IEEE International Symposium on Antennas and Propagation (APSURSI)*. IEEE, 2011, pp. 1185–1188.

[12] W. Huang, Y. He, W. Li, L. Zhang, and S.-W. Wong, "A compact broadband circularly polarized spiral antenna for conformal applications," in *2021 IEEE International Symposium on Antennas and Propagation and USNC-URSI Radio Science Meeting (APS/URSI)*. IEEE, 2021, pp. 1199–1200.

[13] T. Peng, J. L. Volakis, and S. Koulouridis, "Miniaturization of conical helical antenna via optimized coiling," *The Applied Computational Electromagnetics Society Journal (ACES)*, pp. 452–458, 2011.

[14] T. A. Milligan, *Modern antenna design*. John Wiley & Sons, 2005.

[15] A. Ernest, "A deployable bottom fed conical log-spiral antenna for cubesat applications," 2012.

[16] T. M. Apostol and M. A. Mnatsakanian, "Unwrapping curves from cylinders and cones," *The American Mathematical Monthly*, vol. 114, no. 5, pp. 388–416, 2007.

[17] L. Song and Q. Fang, "A conformal conical archimedean spiral antenna for uwb communications," *Chinese Journal of Electronics*, vol. 24, no. 2, pp. 402–407, 2015.

[18] F. W. Grover, *Inductance calculations: working formulas and tables*. Courier Corporation, 2004.

[19] M. Nosrati, A. Jafargholi, R. Pazoki, and N. Tavassolian, "Broadband slotted blade dipole antenna for airborne uav applications," *IEEE Transactions on Antennas and Propagation*, vol. 66, no. 8, pp. 3857–3864, 2018.